.

The Oceanic Surface Layer: Air-Sea Fluxes, Surface Currents, and Material Distributions

1. Air-Sea Momentum and Buoyancy Flux (again)

2. Ekman Boundary Layer (wind stress)

3. Convective Boundary Layer (surface cooling & evaporation)

4. Langmuir Boundary Layer (surface waves & wind)

5. Life in the Euphotic Zone & Air-Sea Gas Flux (next lecture set)

.

Concept: The layer adjacent to the surface has a high level of small-scale (boundary-layer, BL) turbulence.

It's origin is the large vertical gradients in $b(z)$ and $\mathbf{u}(z)$ that arise due to surface buoyancy and momentum fluxes. Whenever the local Richardson number,

$$Ri = \frac{\partial_z b}{(\partial_z \mathbf{u})^2} \lesssim 1,$$

these profiles are unstable and generate turbulence.

Averaged over the turbulent fluctuations, the BL exhibits variability on many scales, primarily controlled by atmospheric variability scales: diurnal, synoptic, seasonal, inter-annual. From this perspective it is reasonable to view it as horizontally homogeneous ($i.e.$, the so-called boundary layer approximation with $\nabla \ll \partial_z$).

Oceanic surface buoyancy and current gradients ($\nabla b,\ \nabla \mathbf{u}$) at mesoscales ($< 100$ km) and submesoscales (< 10 km) disrupt this homogeneity.

Important back effects on the atmosphere occur through surface gravity waves, surface temperature gradients, and surface currents.

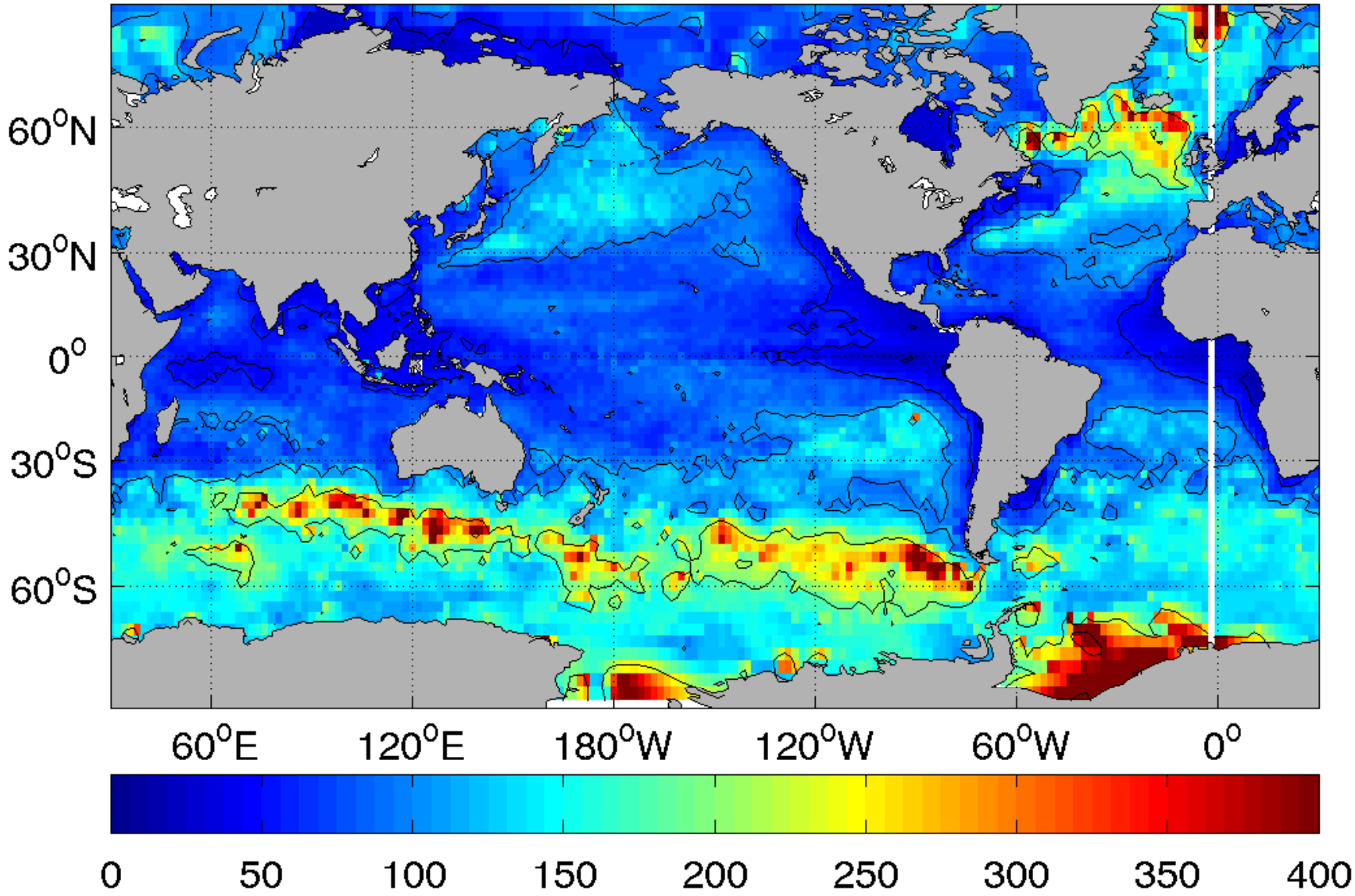

Maximum monthly mean depth h_s [m] of the mixed layer, estimated from climatological profiles of T, S (de Boyer *et al.*, 2004). The mixed layer is operationally (and variously) defined as the depth to which turbulent mixing homogenizes the density of the boundary layer. Boundary layers are shallower in the tropics deeper in subpolar winter regimes. Notice in particular the large values of h_s where abyssal waters form in the far North Atlantic and around Antarctica.

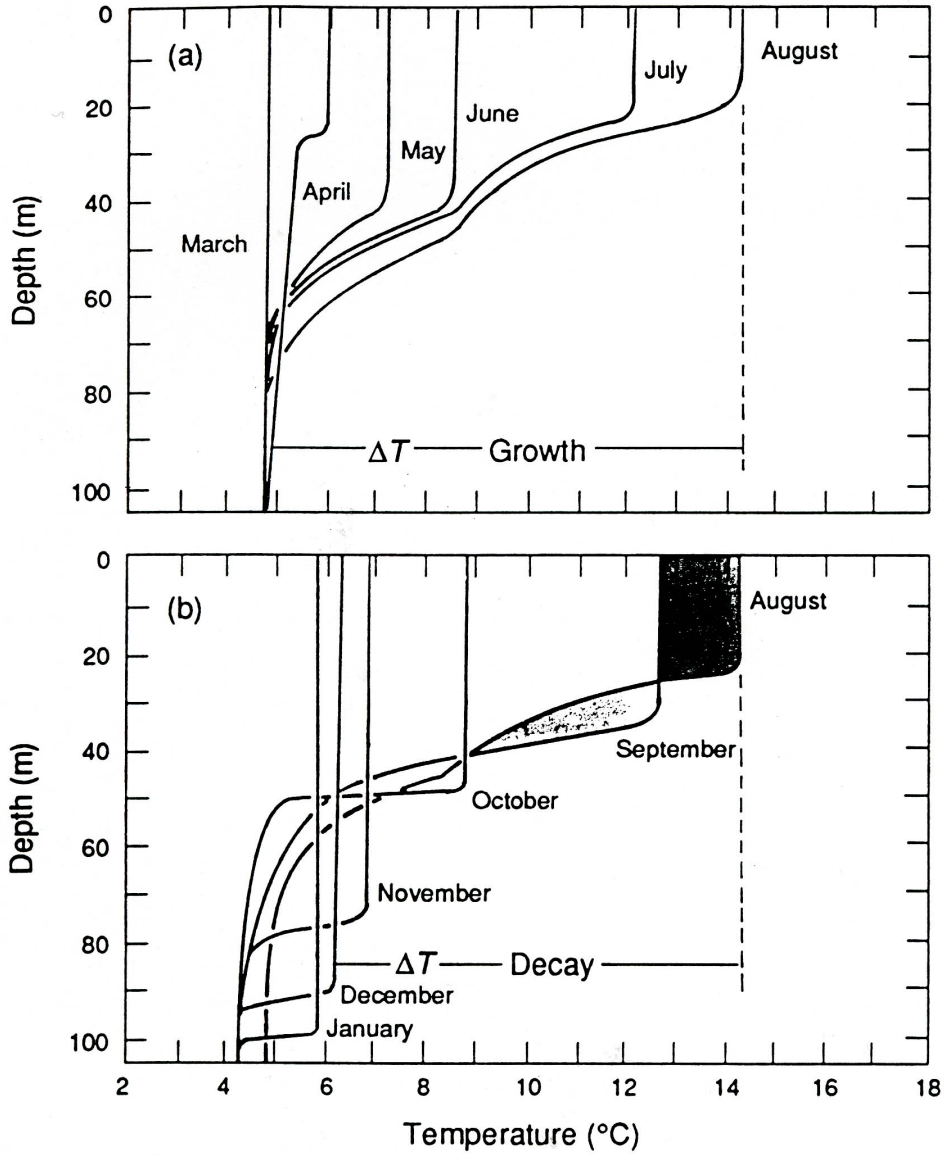

The development of the seasonal thermocline in the eastern North Pacific in the vicinity of 50°N, 145°W. The warming of SST from March to August is due to progressively warmer layers being formed during net heating of the ocean. The cooling from August to September is due to vertical mixing, because equal volumes of cold and warm water are exchanged vertically. Cooling of this area sets in from October onward (Tully and Giovando, 1963).

Annual cycle of the mean temperature profile and mixed layer in the Eastern North Pacific. [Station P; Niiler, 1992]

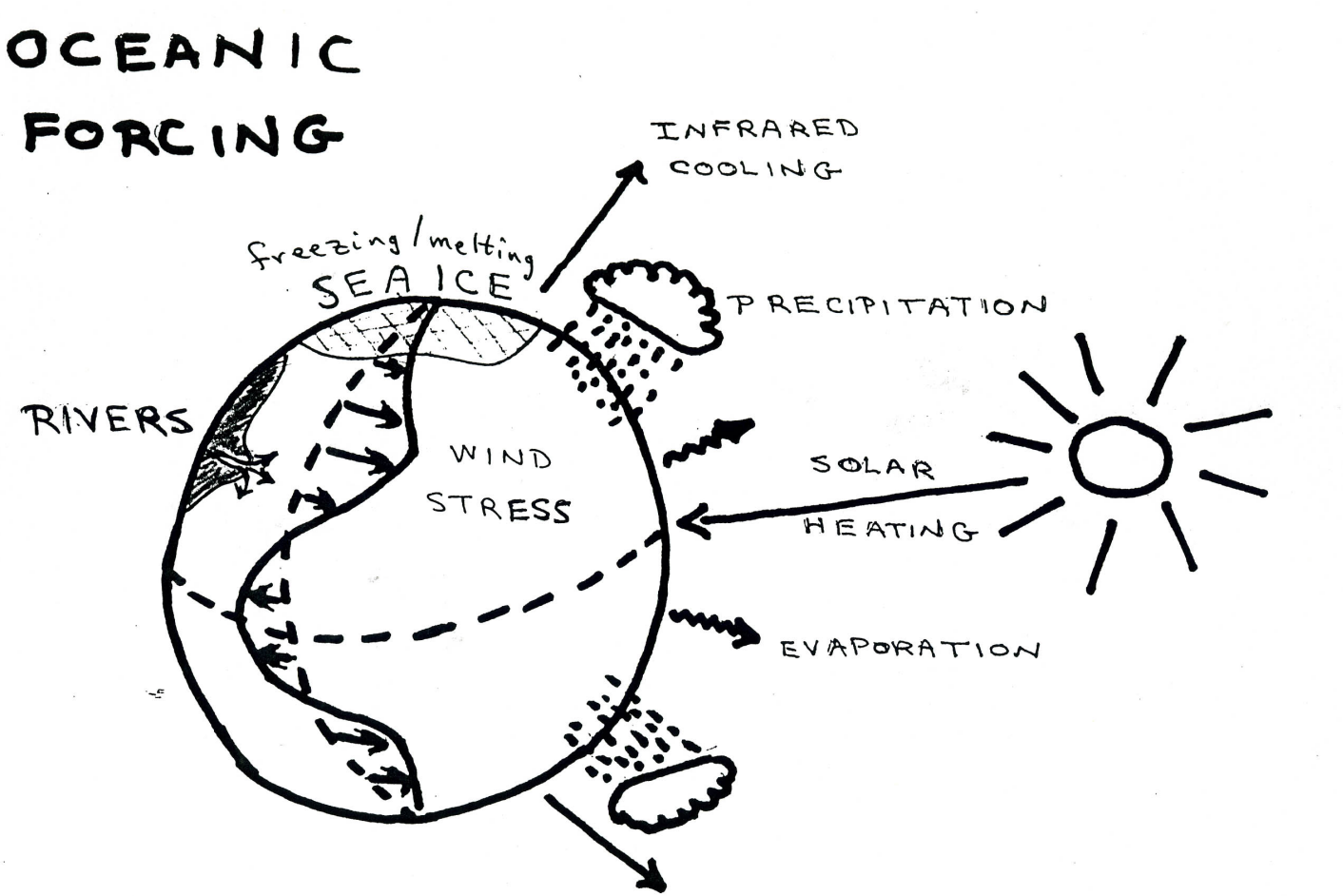

Cartoon of primary momentum, heat, and water forcings of the oceanic circulation. Fluxes are measured and inferred by many techniques. A common approach for stress is evaluated from the near-surface wind $\mathbf{U}_{atm}$ by a bulk formula,

$$\tau^s \;=\; -\,\rho_{atm}\lim_{z\to 0+}[\overline{\mathbf{u}'_h w'}(z)] \;=\; \rho_{atm} C_D^s |\mathbf{U}_{atm}|\mathbf{U}_{atm} \;=\; \rho_o u_*^2\,, \tag{1}$$

with $C_D = \mathcal{O}(10^{-3})$ the empirically calibrated drag coefficient for wind over waves, a moderately increasing function of $|U_{atm}|$ and u_* the "friction velocity" (for turbulence). There are analogous bulk formulae for evaporation and sensible heat flux.

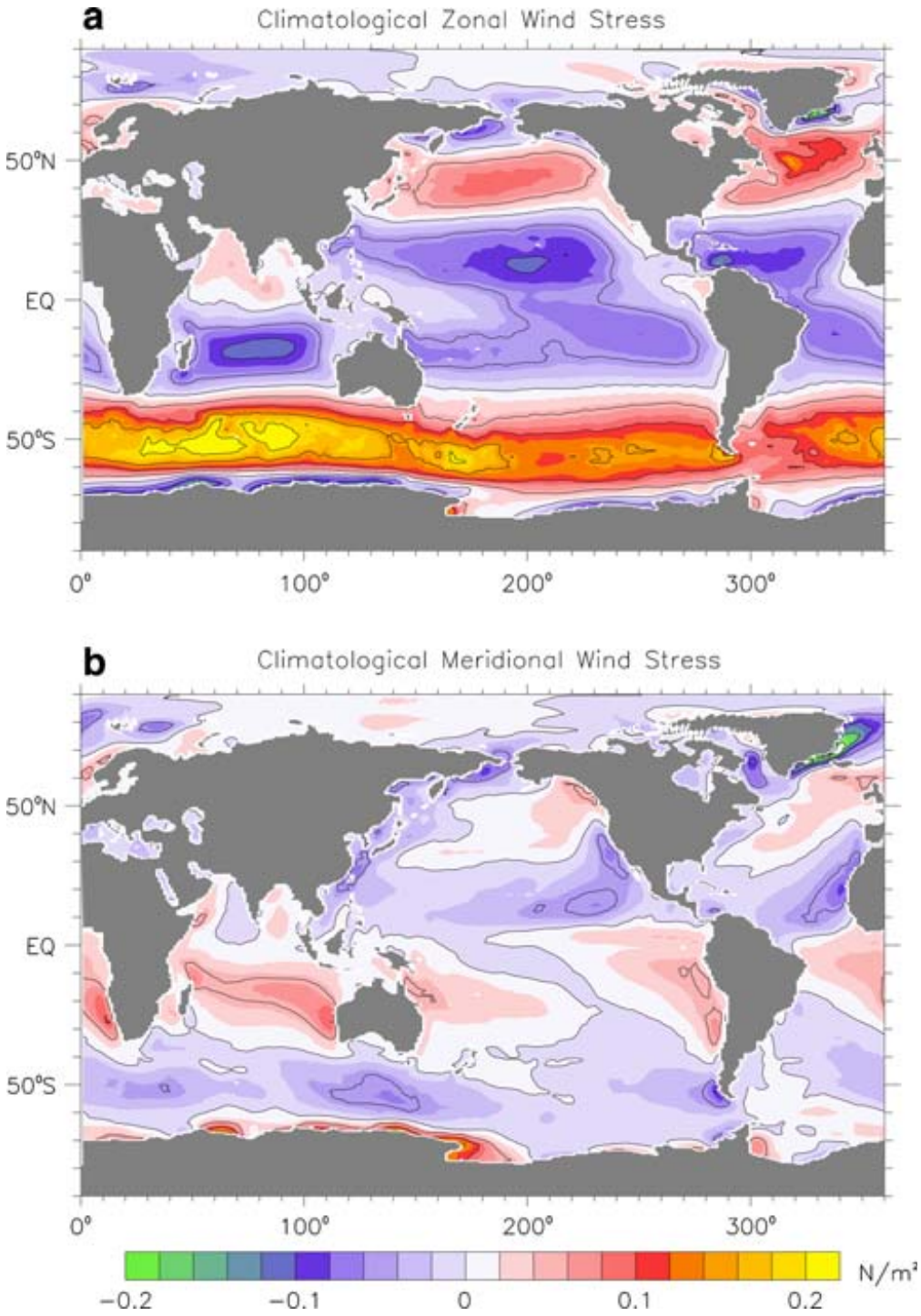

Mean wind stress: (top) zonal, with eastward wind stress on the ocean positive; (bottom) meridional, with northward stress positive. Colored at 0.02 N m^{-2} intervals, with 0.05 N m^{-2} contour intervals. This is a repeated figure. (Large and Yeager, 2009)

For turbulent mixing in the the surface layer, the transient wind stress events are even more important than the mean, *e.g.*, in storms.

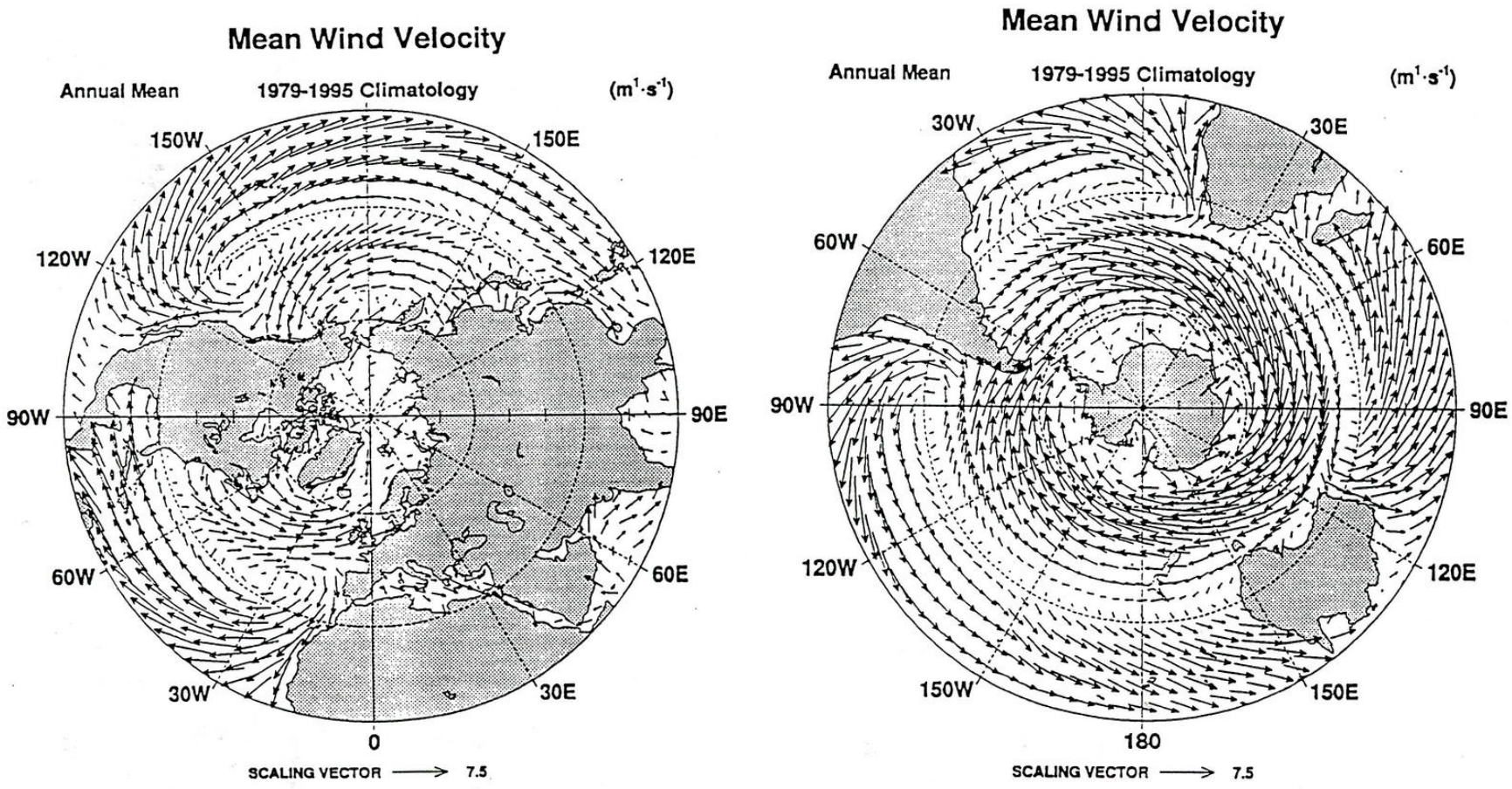

Annual-mean surface wind vector [m s^{-1}] from the NCAR-NCEP reanalysis. (Kalnay *et al.*, 1996)

In this nearly-area-preserving plot, the spatial extent of the easterly trade winds is much broader than the westerlies. The trades generally have milder storm events than the westerlies, except for tropical cyclones.

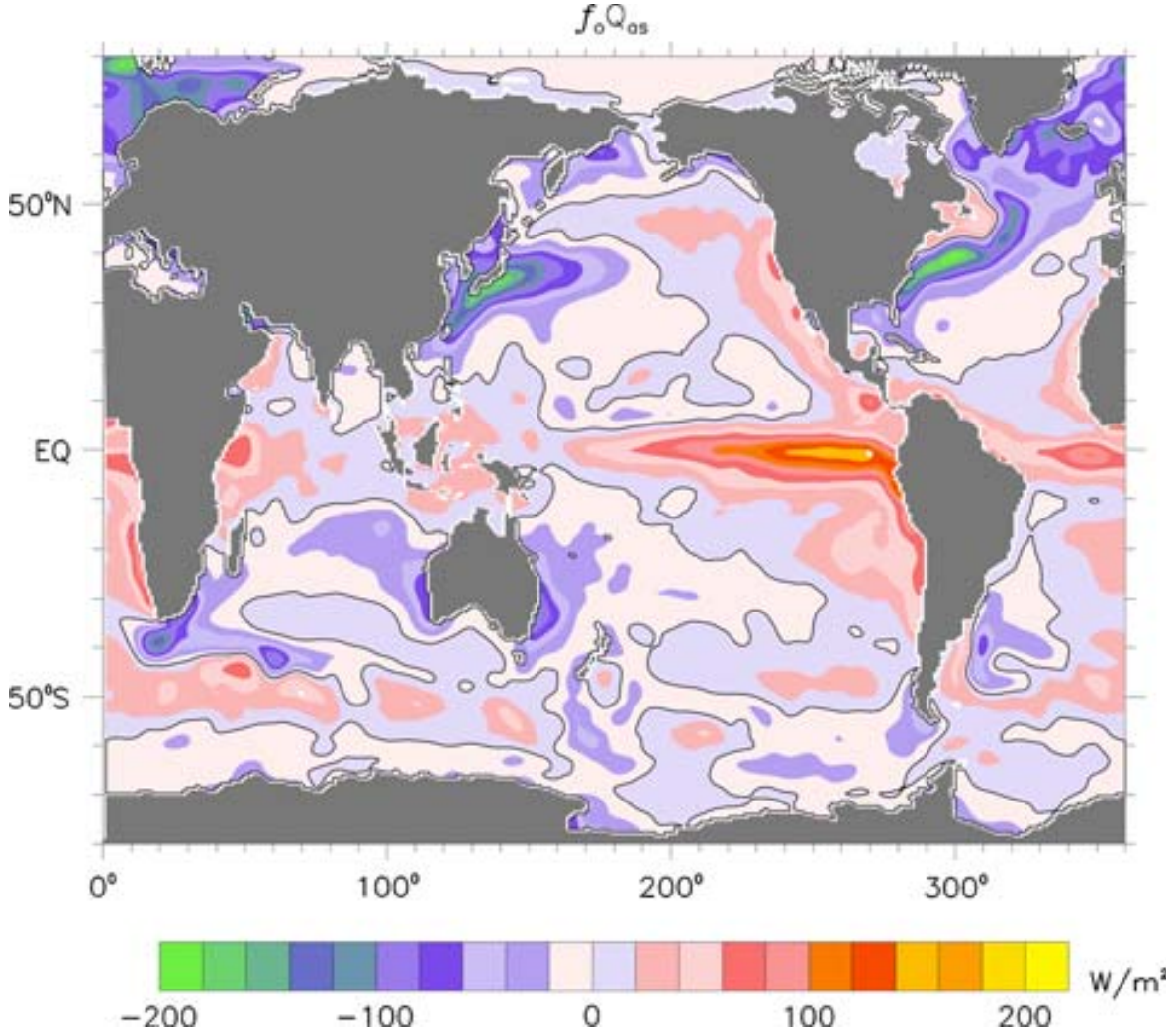

Mean surface heat flux, positive into the ocean, colored at 20 W m^{-2} intervals. (Large and Yeagar, 2009) This figure is also repeated.

$$Q = solar\ warming - infrared\ cooling - latent\ cooling \pm sensible\ heating\,.$$

Transient cooling events are important for turbulent mixing, especially convection.

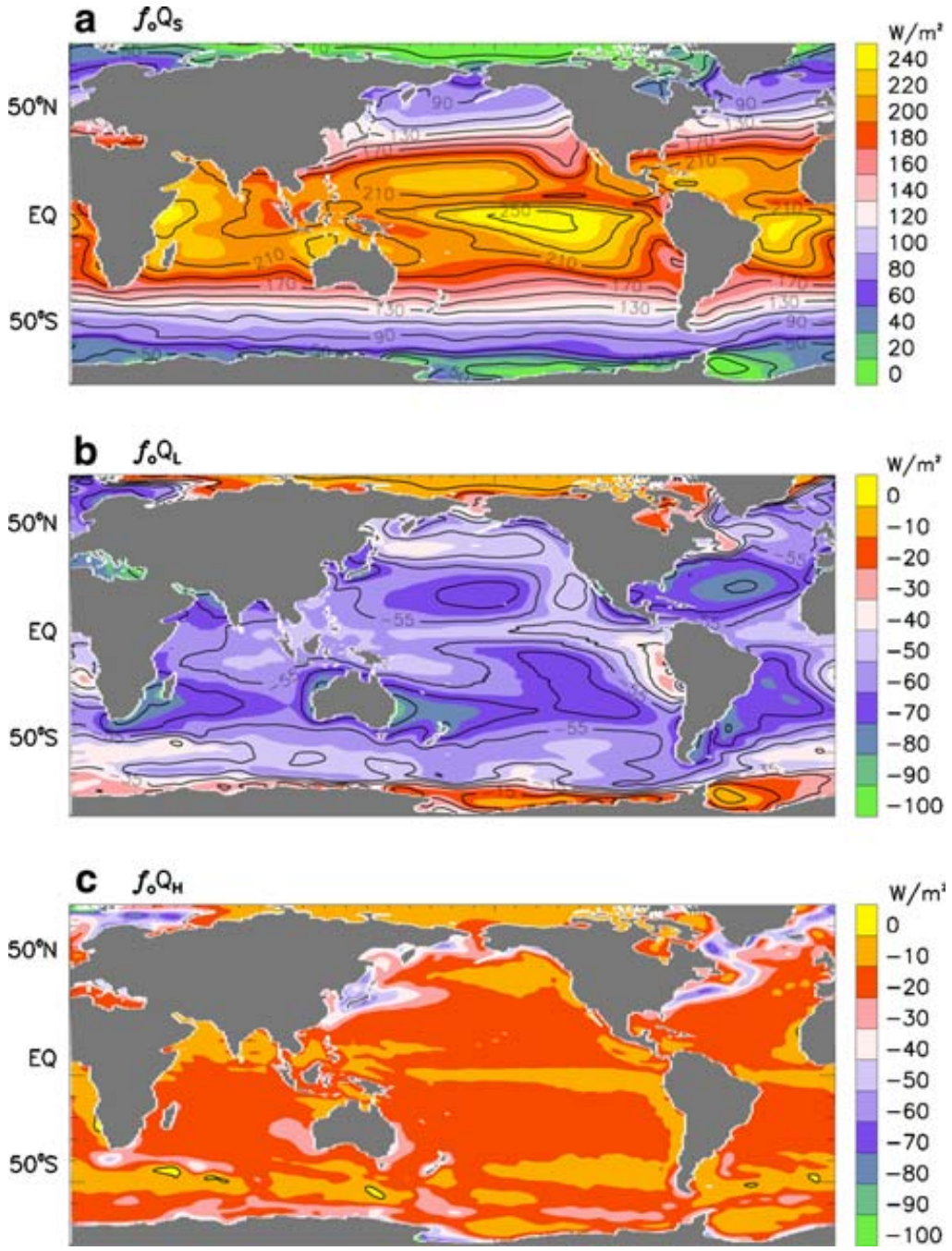

Mean air-sea heat flux components: (a) net solar radiation, with 20 W m^{-2} contour intervals; (b) net long-wave radiation, with 10 W m^{-2} contour intervals; (c) sensible heat flux, with coloring at 10 W m^{-2} intervals. The latent heat flux [W m^{-2}] can be inferred by multiplying the evaporation in Slide 9c by a factor of 2.5 W s mg^{-1}. (Large and Yeagar, 2009)

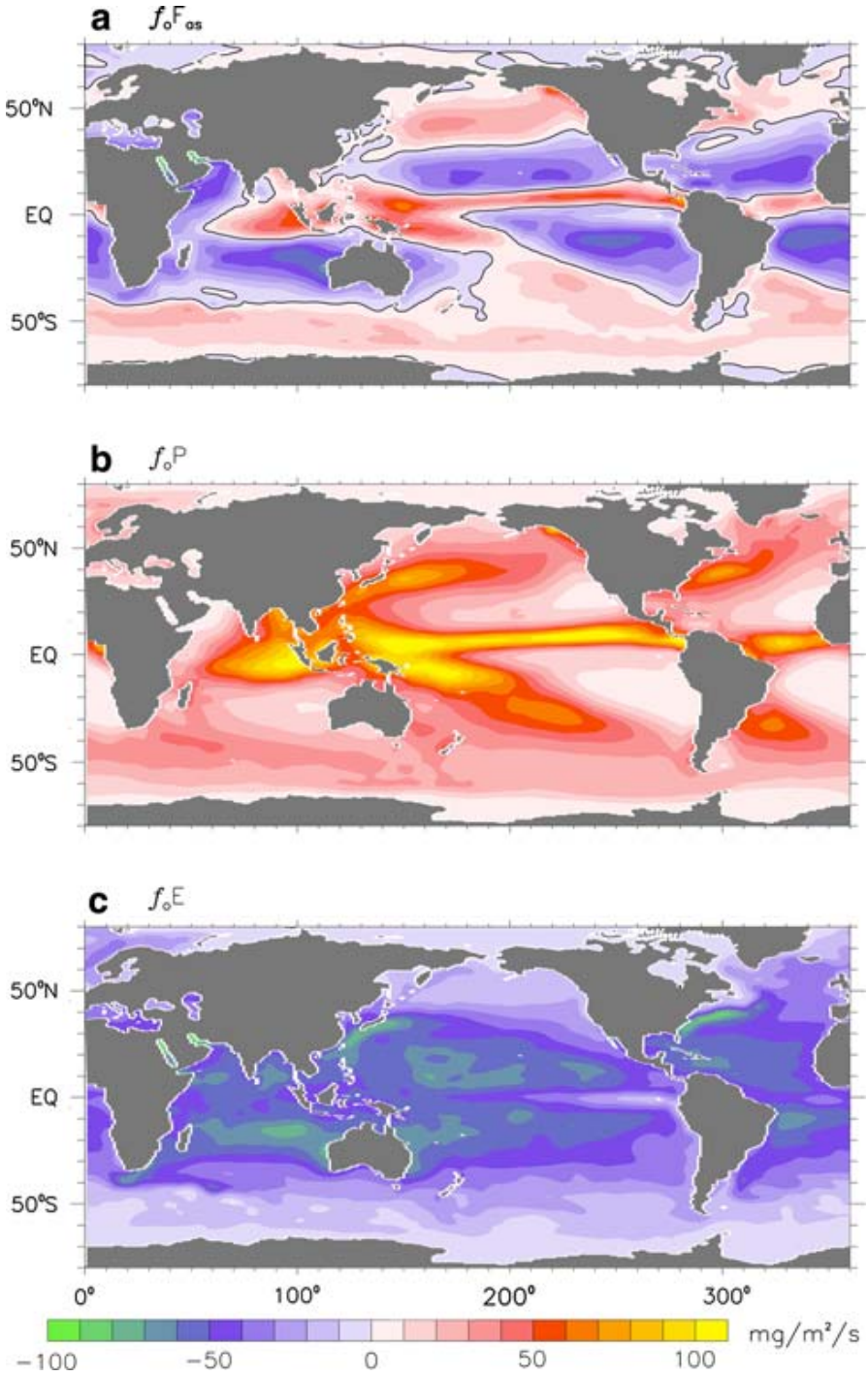

Surface water flux (positive into the ocean):

$$\begin{aligned} \mathcal{F} &= precipitation \\ &\quad - evaporation \\ &\quad + river \\ &\quad \pm seaice\,. \end{aligned}$$

Mean surface water flux, positive into the ocean: (a) total $\mathcal{F}$, (b) precipitation, and (c) -evaporation, colored at 10 mg m^{-2} s^{-1} intervals with a zero contour.

An evaporation rate of 75 mg m^{-2} s^{-1} is equivalent to a cooling of 190 W m^{-2}.

.

Concept: One common type of BL is the shear boundary layer, often called the Ekman layer.

Its origin is the wind over the surface that drags against the ocean, usually with a wavy interface that makes "form stress" (horizontal pressure force against the tilted wave surface) the primary momentum flux from air to water.

The momentum flux is usually interpreted as a wind stress τ that accelerates currents near the boundary, even though surface gravity waves are the physical intermediary between winds and currents.

In a first approximation, the wind speed U_{atm} determines $\mathbf{tau}$, although this assumes that the surface waves have come into local wind-wave equilibrium, and even then a more fundamental view is that $U_{atm} - U_{oce}$ determines τ.

Compared to "laboratory" shear flows, an Ekman layer is different because its boundary stress is not entirely self-determined (see preceding remark), Coriolis force matters, and interior stratification often matters.

Ekman Boundary Layer

Equilibrium momentum balance in an Ekman layer:

$$f\hat{\mathbf{z}} \times \overline{\mathbf{u}}_{ek} \;\approx\; -\partial_z \overline{\mathbf{u}'_h w'}\,,$$

with integral transport, $\mathbf{T}^s_{ek} \;\equiv\; \int_{-h_{ek}}^{0} \overline{\mathbf{u}}_{ek}\, dz \;=\; -\frac{1}{f\rho_0}\,\hat{\mathbf{z}} \times \tau^s$.

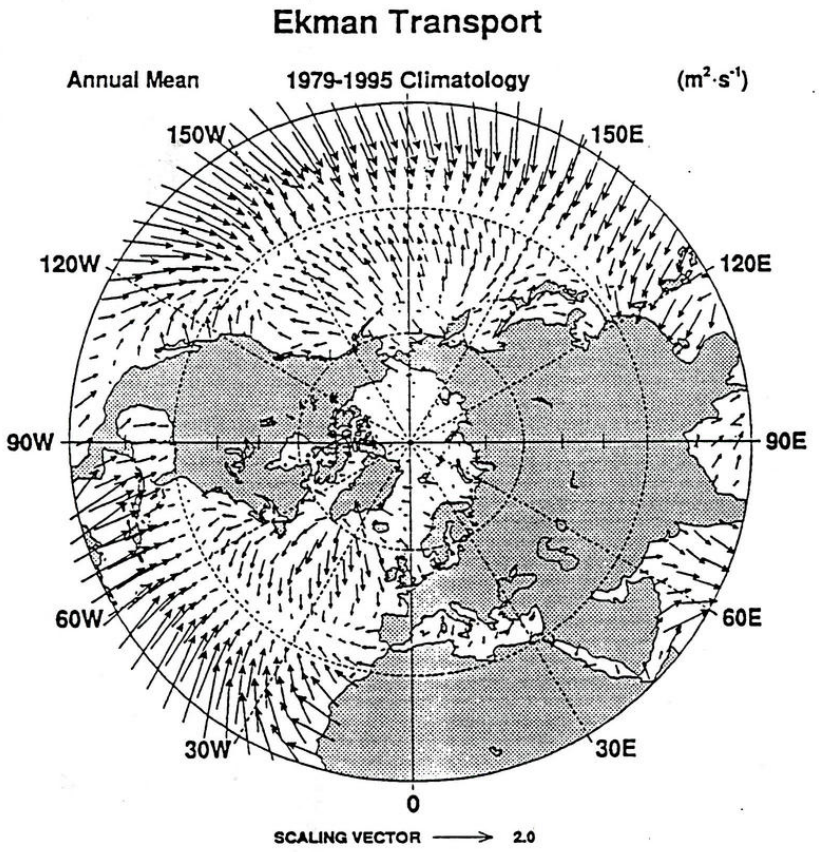

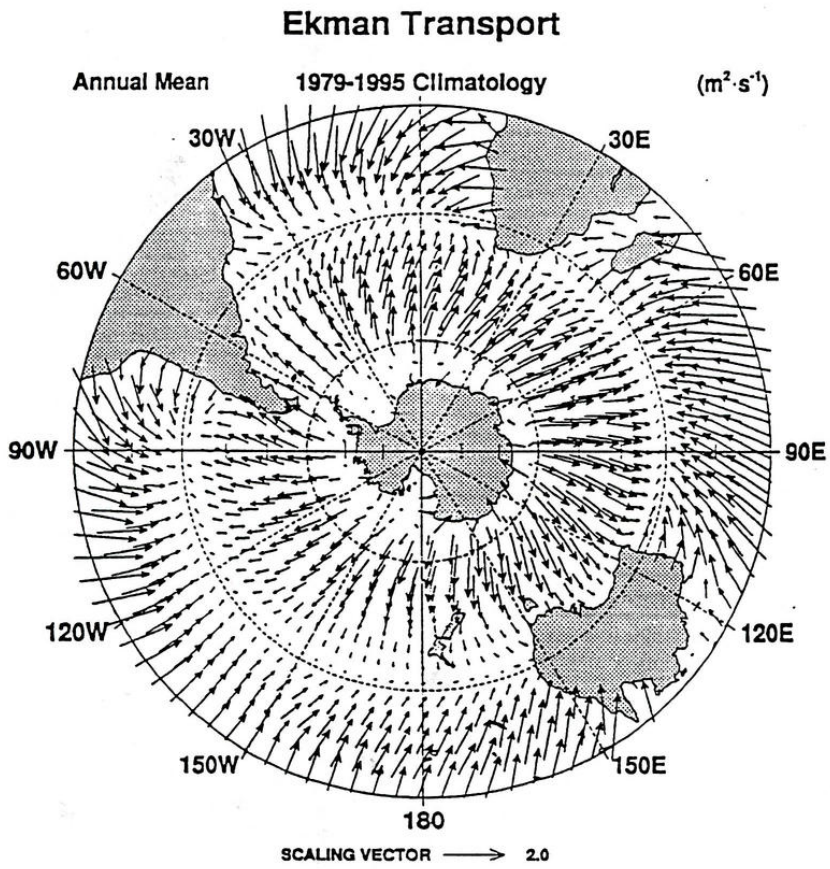

Annual-mean surface Ekman transport, $\mathbf{T}^s_{ek}$ [m^{2}s^{-1}] (McWilliams and Restrepo, 1999), based on the winds from the NCAR-NCEP reanalysis (Kalnay *et al.*, 1996). Notice the equatorial divergence, subtropical convergence, and subpolar divergence, as well as eastern boundary divergence/upwelling.

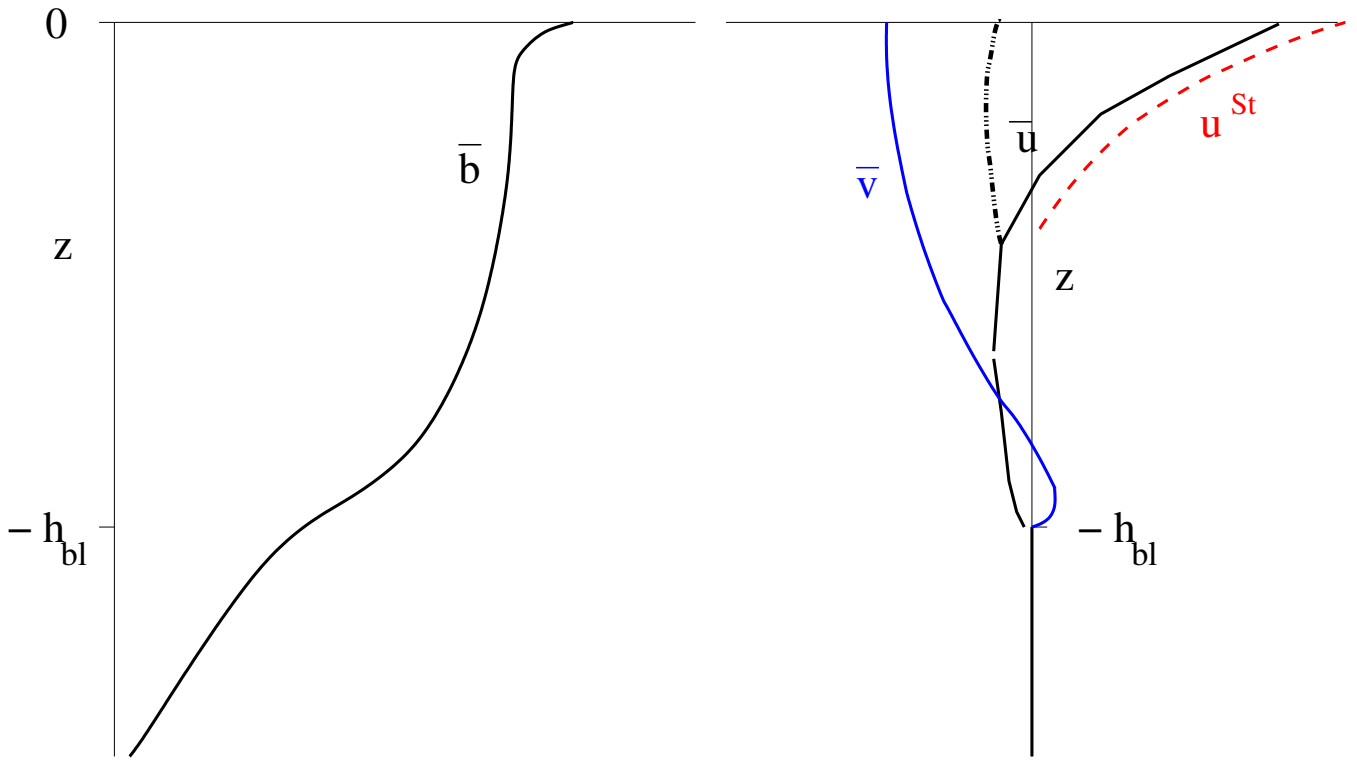

Sketch of surface BL profiles for mean buoyancy $\overline{b}$ and velocity $\overline{\mathbf{u}}$ (solid black and blue lines) for a stratification-limited Ekman BL with $\tau^{s,x} > 0$ and $Q_{os} > 0$. With the additional effects of surface gravity waves and Stokes drift (*i.e.*, in the Langmuir BL; see Slide 18), the $\overline{u}$ profile shifts backward (black dot-dash line) in conjunction with the down-wave, down-wind Stokes drift $\mathbf{u}^{St}(z)$. Note that $\int_{-h_{bl}}^{0} v\, dz = -\tau^{s,x}/f\rho_o$, *i.e.*, the Ekman transport relation.

- unstratified Ekman layer: $h_{ek} \sim u_*/f$ with $u_* = \sqrt{|\tau|/\rho_0}$.
- stratified Ekman layer: $h_{ek} \sim u_*/N$ with $N = \sqrt{\partial_z \overline{b}}$ the adjacent interior buoyancy frequency.

. . . or even a hybrid, $h_{ek} \sim u_*/\sqrt{fN}$ (Ralph and Niiler, 1999).

Turbulent kinetic energy (TKE), $e = \frac{1}{2}\overline{(\mathbf{u}')^2}$, is sustained by mean Ekman flow instability:

$$\partial_t e = shear\ production + buoyancy\ work - dissipation + transport$$

where shear production is $-\overline{\mathbf{u}_h' w'}\,\partial_z \overline{\mathbf{u}}_h$; buoyancy work is $\overline{w'b'}$; and viscous dissipation is $\epsilon = \nu\overline{(\nabla \mathbf{u}')^2}$. In a steady Ekman layer, production approximately balances ϵ, and $\overline{w'b'} < 0$ is a small correction. Transport is a flux divergence that can only rearrange $e(z)$ in the vertical.

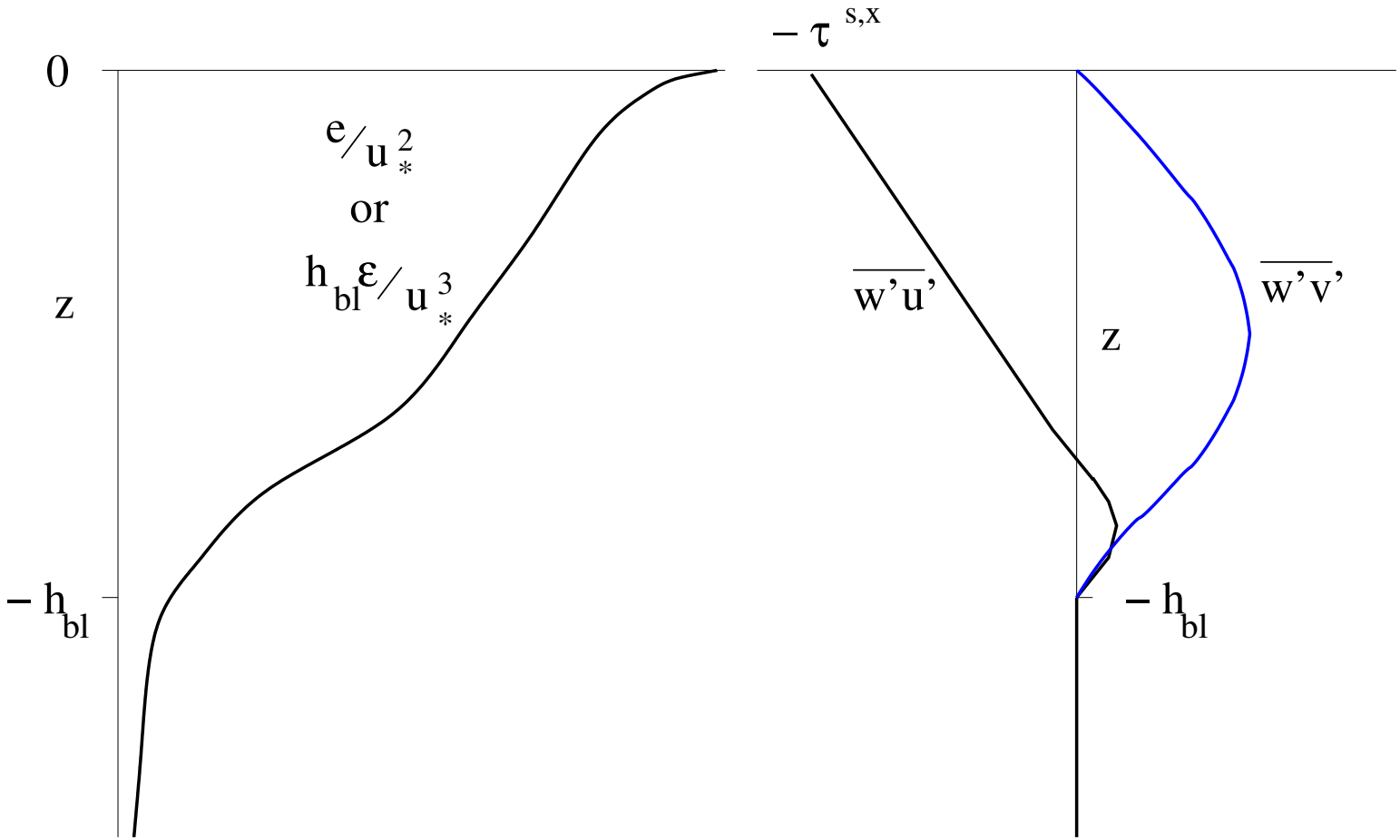

Sketch of surface BL profiles for turbulent kinetic energy e, dissipation rate ϵ, and Reynolds stress components $\overline{w'\mathbf{u}_h'}$ for a stratification-limited Ekman BL with $\tau^{s,x} > 0$.

.

Concept: Another common type of BL is the convective boundary layer.

Its origin is buoyancy loss through the surface due to cooling and/or net evaporation. This creates $\partial_z b < 0$ near the surface, which is gravitationally unstable.

Even in the tropics, the BL is usually convective during a diurnal cycle because evaporative cooling continues through the night after the sun has gone down.

Deep water formation almost always occurs during convective conditions, whether in the open ocean or on a shelf with mixing to the bottom.

When the surface buoyancy flux is stablizing, there usually is enough wind and/or surface waves to keep the BL turbulent, albeit with a reduced layer depth h.

Compared to "laboratory" convection, oceanic convection is usually limited by interior stable stratification, which it erodes by penetrating plumes that $entrain$ adjacent quiescent fluid and cause the boundary layer depth h to progressively increase. Compared to "atmospheric" convection, clouds are not a concern.

Convective Boundary Layer

Mean buoyancy balance in a convective BL with surface cooling $Q = -\overline{w'b'}(0) < 0$:

$$\partial_t \overline{b} \;\approx\; -\partial_z \overline{b'w'}\,,$$

with an e balance, $-Q \;=\; \overline{w'b'} \;\approx\; \epsilon$. During convection $\partial_t h_{bl} > 0$; *i.e.*, BL deepening.

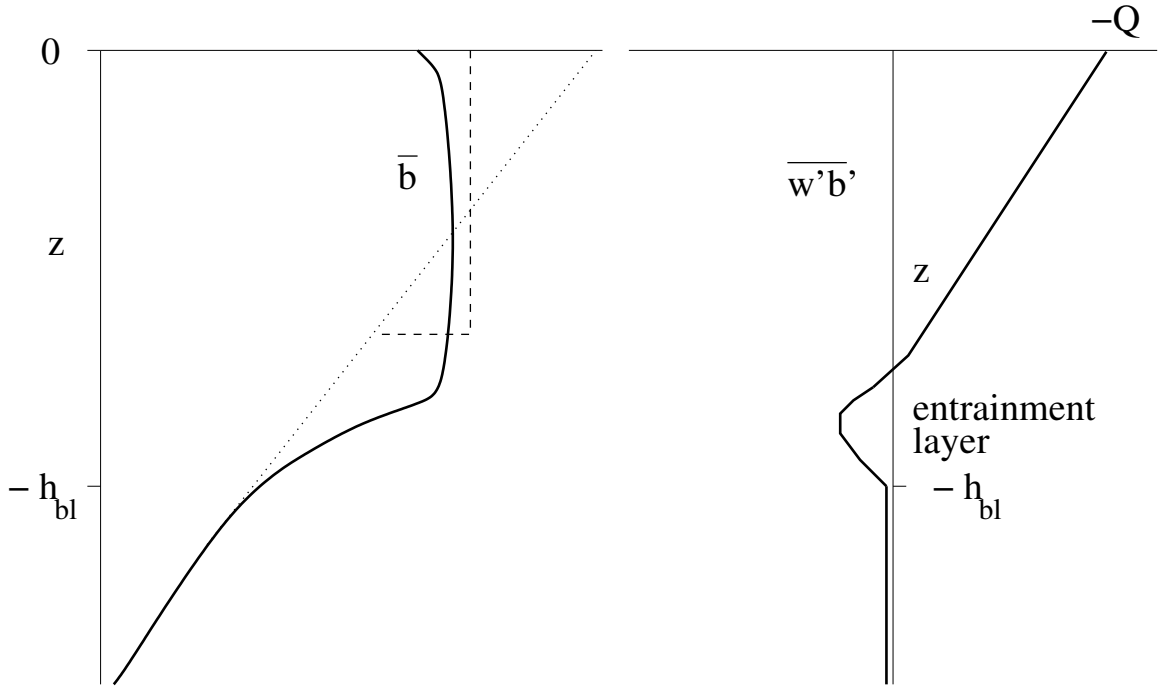

Sketch of BL profiles for mean buoyancy $\overline{b}(z)$ and the turbulent vertical buoyancy flux $\overline{w'b'}$ in penetrative convection. The surface is cooled at a rate $Q < 0$, and there is no surface stress, $\boldsymbol{\tau}^s = 0$. Turbulence carries heat upward ($\overline{w'b'} > 0$) over most of the BL, but it "entrains" colder water from below near the bottom. Dotted line indicates $\overline{b}(z)$ profile before onset of convection. For comparison the dashed line shows what the mean profile would be if there were no entrainment and mixing penetrated only to a minimum depth consistent with net cooling, $\int_0^t Q\,dt < 0$, and stable stratification, $\partial_z \overline{b} \geq 0$.

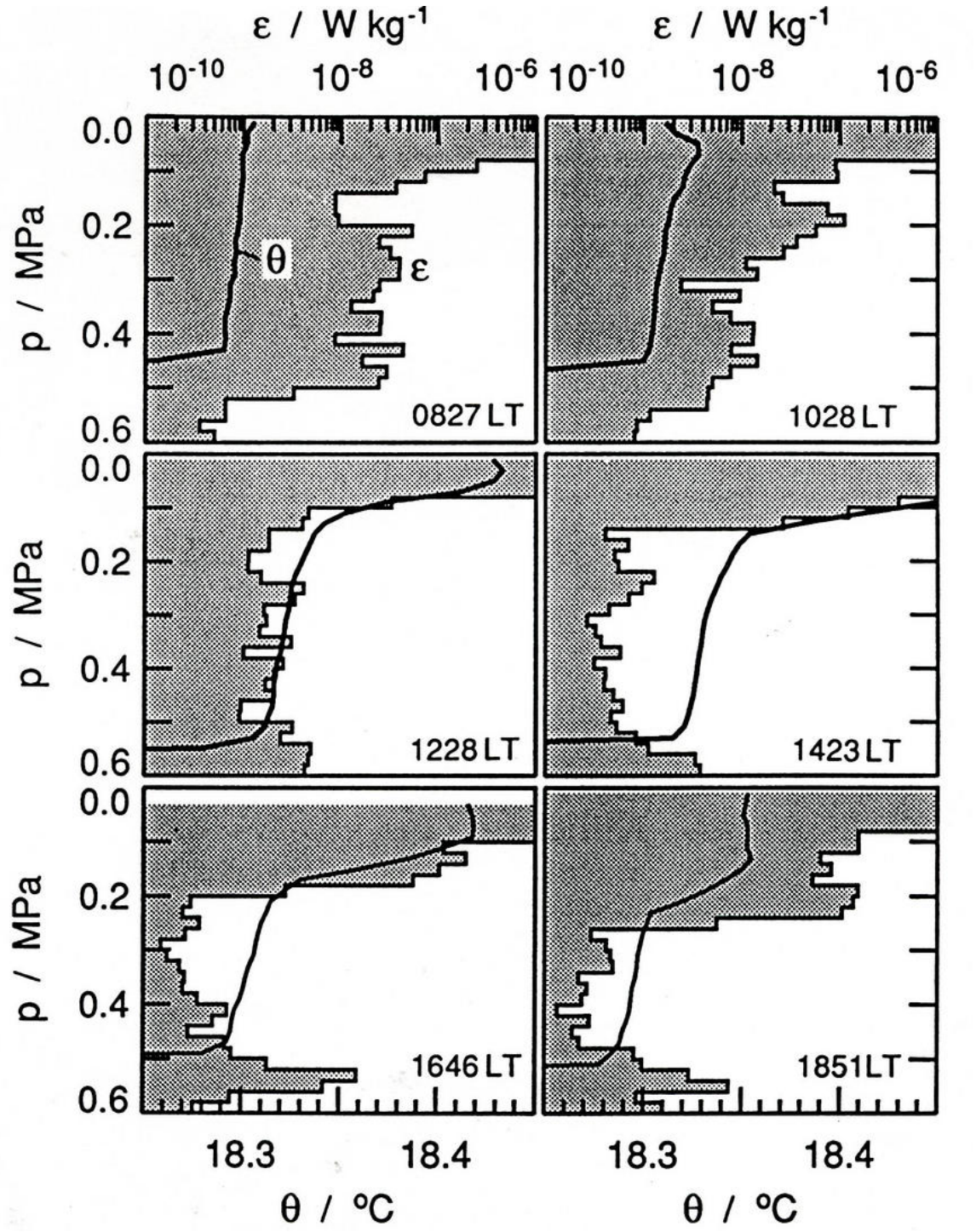

Measured profiles of hour-averaged dissipation rate ϵ (shading) and potential temperature θ (line) through part of a diurnal cycle in the tropics. LT denotes local time, and the depth unit [MPa $= 10^6$ Pa, pressure] is approximately equivalent to 100 m. Overnight infrared cooling induces convection, large h_{bl}, high ϵ, and well-mixed $\theta = T$. During the day shallow solar heating stabilizes the Ekman layer and shrinks h_{bl}. The wind stress is approximately constant throughout the day, so the diurnal cycling is between unstable and stable Ekman layers. (Brainard and Gregg, 1993)

Concept: Usually the ocean surface has wind-generated gravity waves that influence the BL turbulence.

Their origin is the instability of a flat free-surface interface when wind blows over it.

Waves have two different types of effects on the BL: one is to $break$ and thereby transfer momentum and energy from the waves to the currents ($i.e.$, the second step in "wind stress"); the other is to provide $wave\text{-}averaged\ forces\ and\ material\ advection$ by the waves' "eddy-induced velocity", usually called the Stokes drift.

An important concept is $wind\text{-}wave\ equilibrium$, which will develop if a wind is statistically steady for several hours and if there is sufficient "fetch" ($i.e.$, distance from the shoreline). Under these conditions wind-input (wind drag) is equal to wave-output (wave breaking).

Relative to wind-wave equilibrium, other conditions are young waves, old waves, remotely generated swell, and shoreline breaking (surf).

The BL with important wave effects is often called $Langmuir\ turbulence$ in recognition of the coherent structures (wind rows) that arise.

Compared to classical "laboratory" flows, the oceanic wavy BL is just weird.

Langmuir Boundary Layer

When there are surface gravity waves, there is a time-averaged Lagrangian velocity ($i.e.$, following bobbing parcels) even if there is no Eulerian mean velocity ($i.e.$, at a point in space); see Slide 20. The theoretical formula for this Stokes drift velocity is

$$\mathbf{u}^{St}(z) \;\approx\; \langle\, (\int^t \mathbf{u}^w\, dt)\cdot\nabla\,)\,\mathbf{u}^w\,\rangle\,,$$

where $\mathbf{u}^w(x,y,z,t)$ is the instantaneous wave parcel velocity, and the angle brackets denote an average over a wave oscillation period. For example, a simple, single-frequency, deep-water wave with $\eta^w = a\cos[kx-\sigma t]$ (a is amplitude, $2\pi/k$ is horizontal wavelength, and σ is frequency), has a drift profile,

$$\mathbf{u}^{St}(z) \;=\; \frac{a^2\sigma}{2}\,e^{2kz}\,.$$

A typical magnitude of the Stokes drift in wind-wave equilibrium is $|\mathbf{u}^{St}|(0) \;=\; 10u_*$; $i.e.$, a **Langmuir number**, $La = \sqrt{u_*/U^{st}} \approx 0.3$. For $U_{atm} = 10$ m s^{-1} and $a = 1$ m, a typical wavenumber scale for the peak of the surface wave spectrum in $k \;=\; 2\pi/75$ m $\approx\; 0.08$ m^{-1}; hence, a typical depth scale for $\mathbf{u}^{St}$ is $1/2k \;\approx\; 6$ m, usually shallower than the BL depth h_{bl}.

A steady Langmuir BL has

- Unstratified layer: $h_L \;\sim\; u_L/f$ with $u_L \sim \sqrt{u_*^2 + c\,(\mathbf{u}^{St})^2}$, with $c \approx 0.03$.
- Strong interior stratification: $h_{bl} \;\sim\; u_L/N$.

$\mathbf{u}^{St}(z)$ and $\mathbf{u}(z)$ are sketched in red in Slide 13.

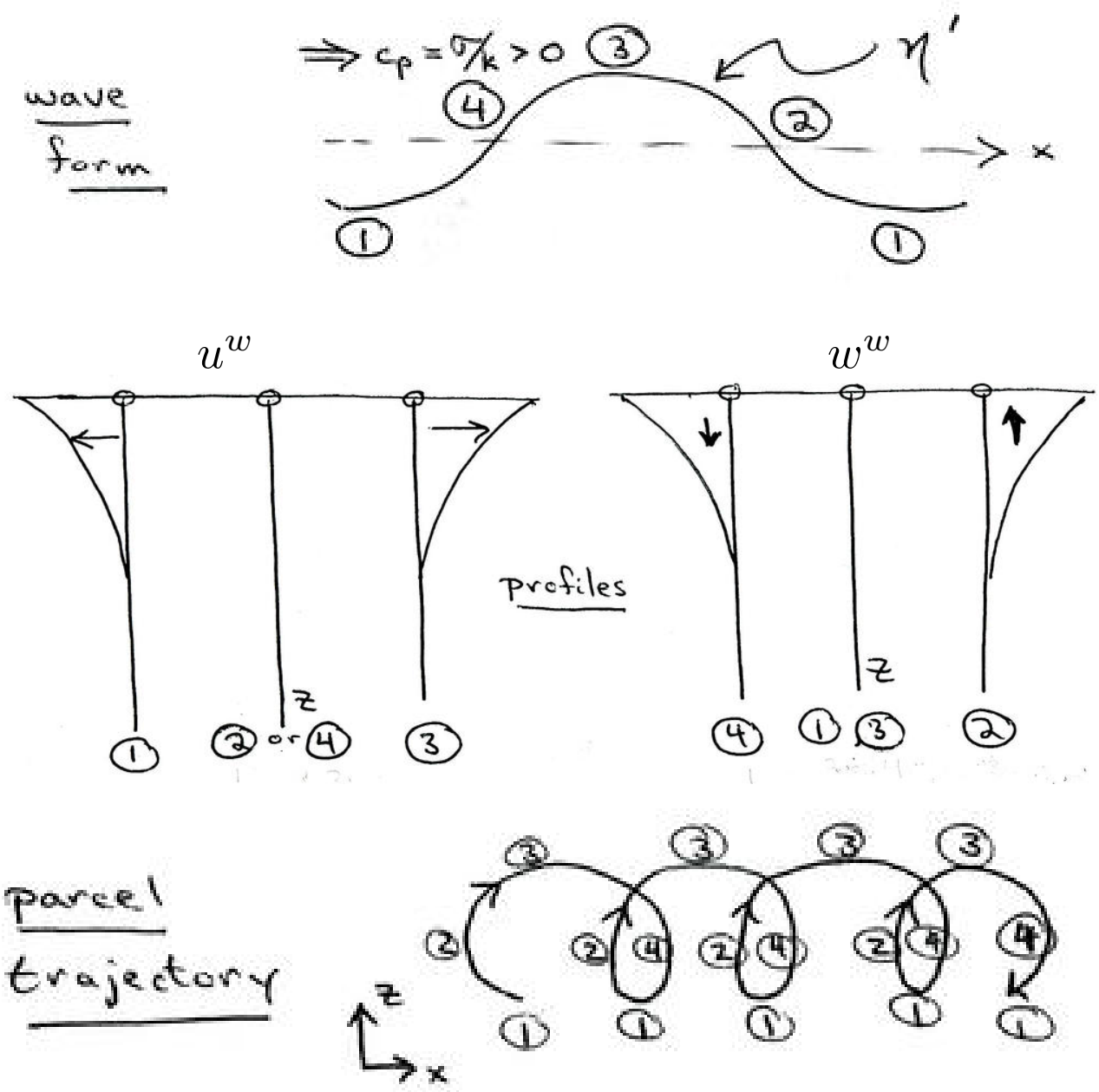

Cartoon of surface gravity wave motion and Stokes drift. Top panel: the surface elevation with circled numbers marking phases of the oscillation. Middle panel: horizontal and vertical velocity profiles at particular phases. Bottom panel: a parcel trajectory over many oscillation cycles.

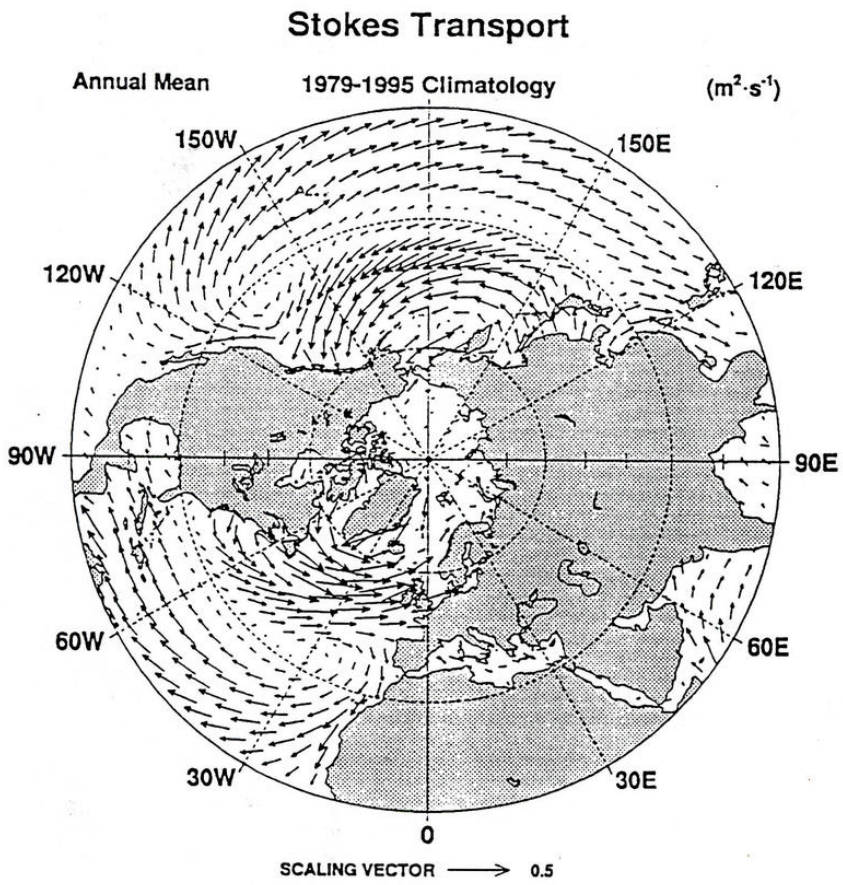

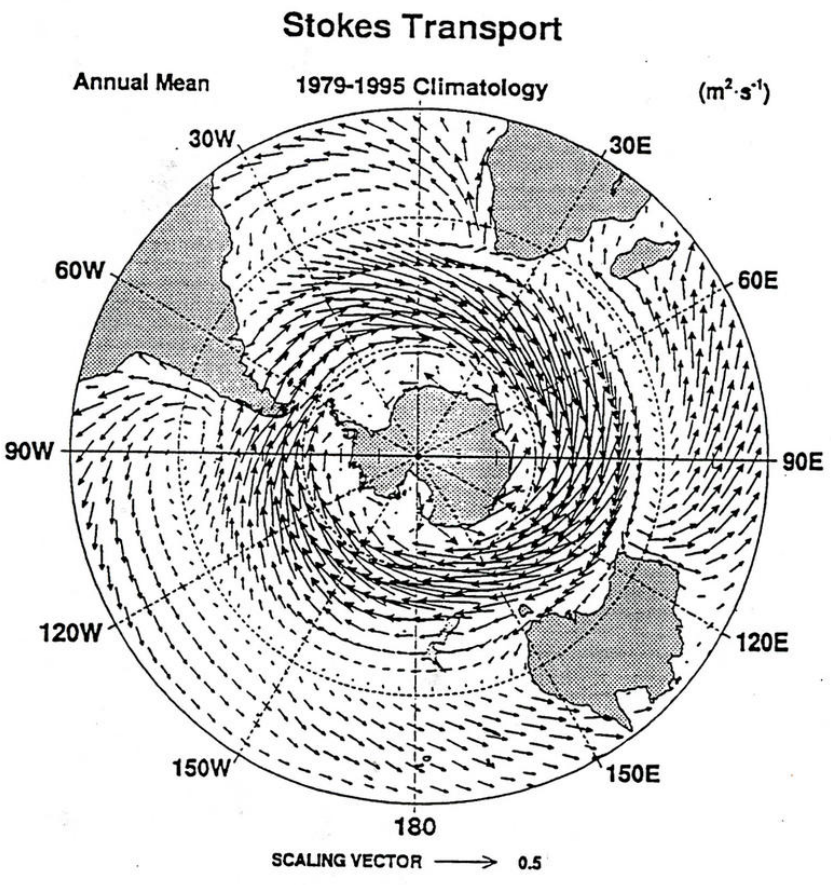

Annual-mean Stokes transport, $\mathbf{T}_{st} = \int \mathbf{u}^{St}\, dz$ [m^{2}s^{-1}] (McWilliams and Restrepo, 1999).

This analysis is on the winds from the NCAR-NCEP reanalysis (Kalnay $et\ al.$, 1996) and the assumption of wind-wave equilibrium.

$\mathbf{T}_{st}$ is directed downwind because the waves are. It is larger in higher latitudes where winds are stronger.

When waves and currents occur together, $\mathbf{u}^w + \mathbf{u}$, we can derive a theory for the wave-averaged dynamical effects of the waves on the currents, buoyancy, and other materials. The important results for the Boussinesq equations (*cf.*, Dynamics Lecture) are

$$\begin{aligned} \frac{D\mathbf{u}}{Dt} + 2\boldsymbol{\Omega} \times \mathbf{u} &= -\nabla\phi - \frac{g}{\rho_0}(\rho - \rho_0)\hat{\mathbf{z}} + \mathcal{D}[\mathbf{u}] - (\nabla \times \mathbf{u}) \times \mathbf{u}^{St} - 2\boldsymbol{\Omega} \times \mathbf{u}^{St} \\ \frac{Db}{Dt} &= \mathcal{D}[b] - \mathbf{u}^{St} \cdot \nabla b \,, \end{aligned}$$

with an equation for material C analogous to that for b. Notice the three new terms $\propto \mathbf{u}^{St}$. They are respectively called the vortex force, Stokes-Coriolis force, and Stokes tracer advection. The interpretation is that both vortex-lines and materials move with the Lagrangian mean velocity,

$$\mathbf{u}^L = \mathbf{u} + \mathbf{u}^{St} \,,$$

which is the sum of the wave-averaged Eulerian current and the Stokes drift.

Equilibrium momentum balance in an Langmuir-Ekman layer with surface stress τ^s and Stokes drift $\mathbf{u}^{St}(z)$:

$$f\hat{\mathbf{z}} \times (\overline{\mathbf{u}}_h + \mathbf{u}^{St}) \approx -\partial_z \overline{\mathbf{u}'_h w'} \,,$$

with an integral transport relation for the Eulerian Ekman current current,

$$\mathbf{T}^s_{bl} = -\frac{1}{f\rho_0}\hat{\mathbf{z}} \times \tau^s - \mathbf{T}^{St} \,.$$

The Lagrangian (material) transport is still normal to the stress, but the Eulerian transport has an upwind component.

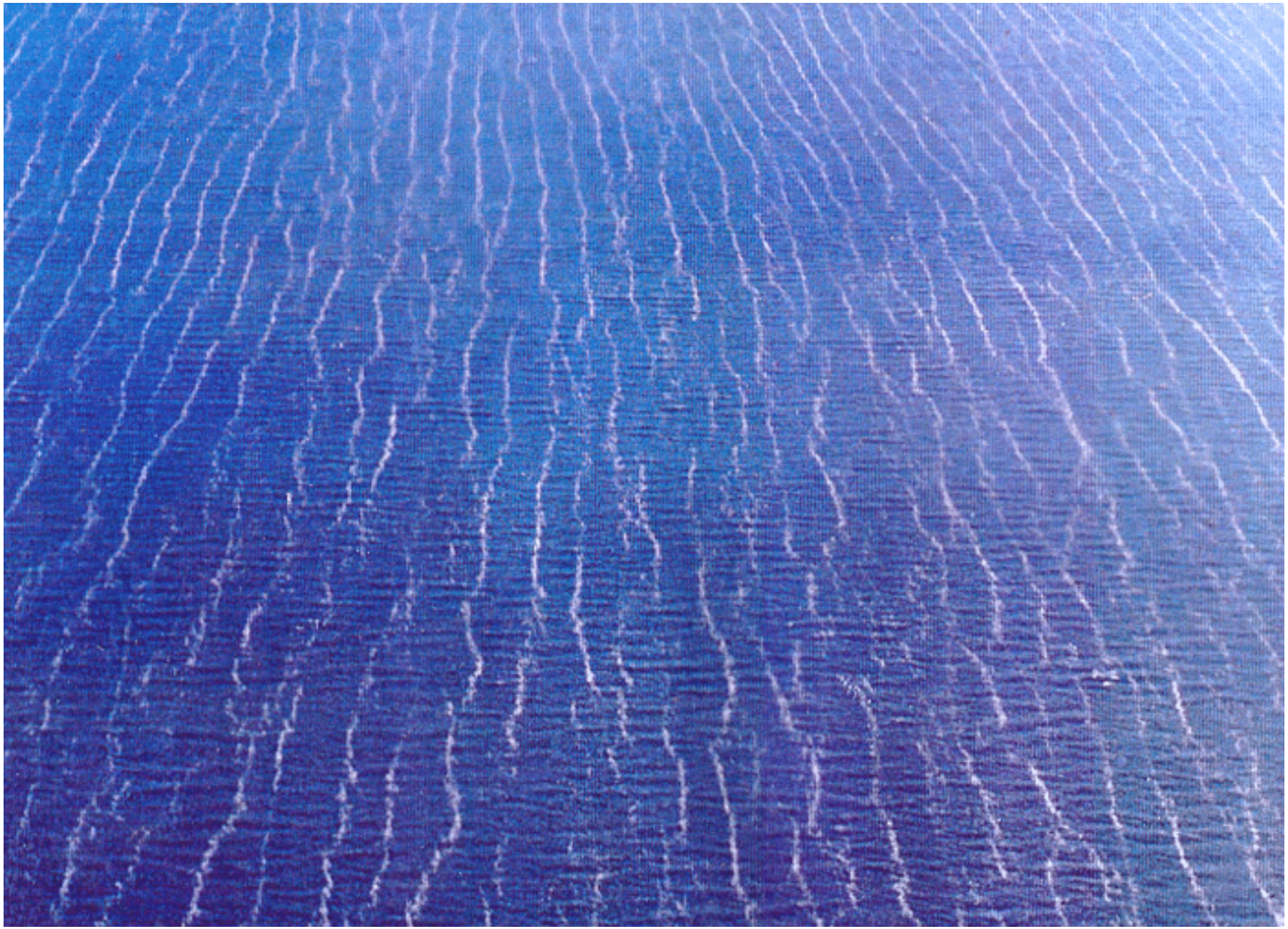

Photograph of converging foam lines generated by Langmuir circulations in the Great Salt Lake also called wind rows. Notice the surface wave crests perpendicular to the foam lines. The oceanic surface is often dirty with biogenic buoyant surfactants (scum). (Sullivan and McWilliams, 2010)

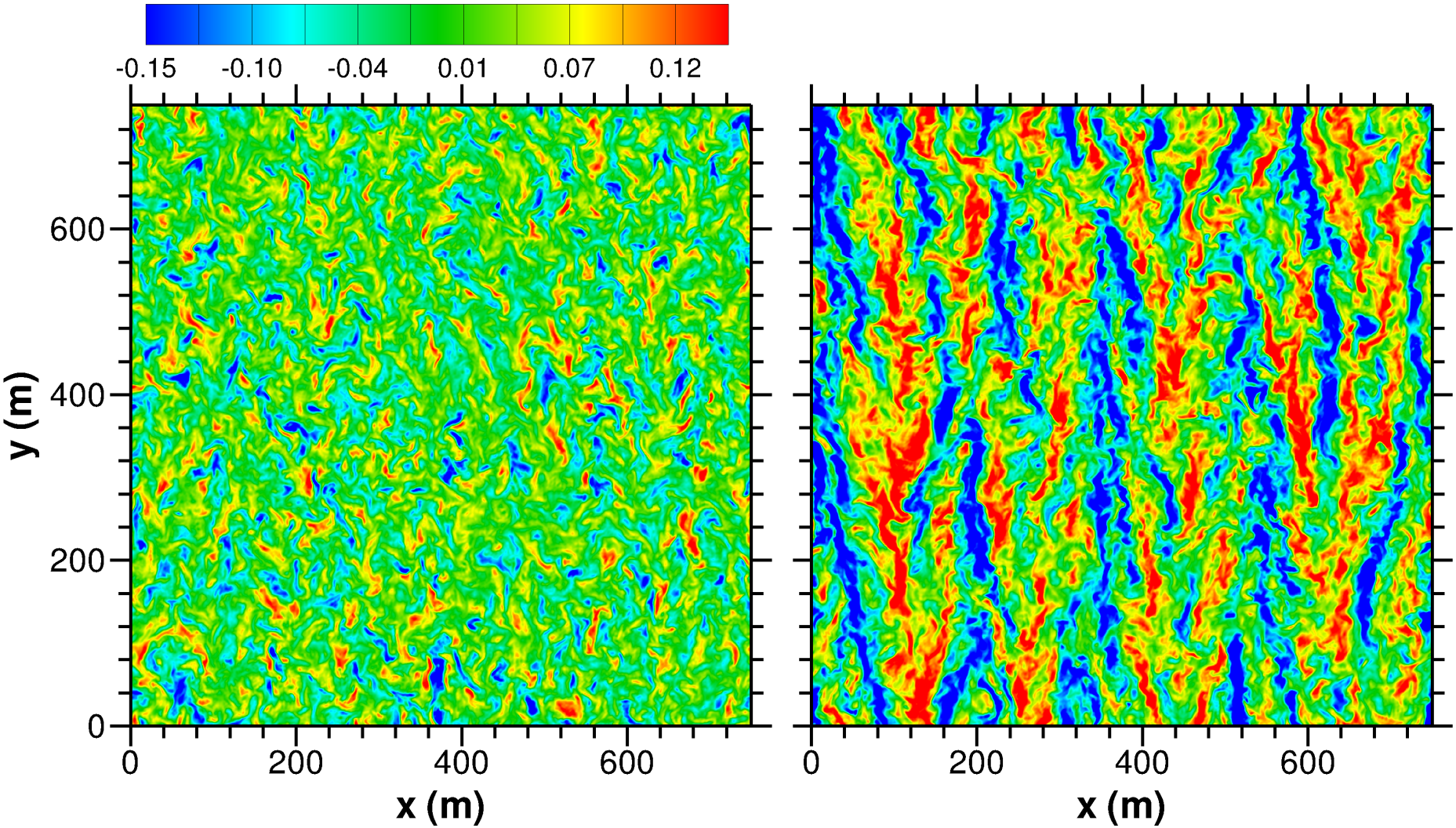

Snapshot in a Large-eddy computational simulation of the turbulent BL under a hurricane of $w(x, y)$ [m s^{-1}] at $z = -30$ m with northward wind with (right) and without (left) including the wave-dynamical influence of the vortex force. Notice the turbulent Langmuir circulations (LCs) approximately aligned with the Stokes drift in the right panel, and w is much stronger. When LCs occur ($i.e.$, when surface waves are strong), they greatly enhance the vertical mixing and transport efficiency. (Sullivan and McWilliams, 2010)

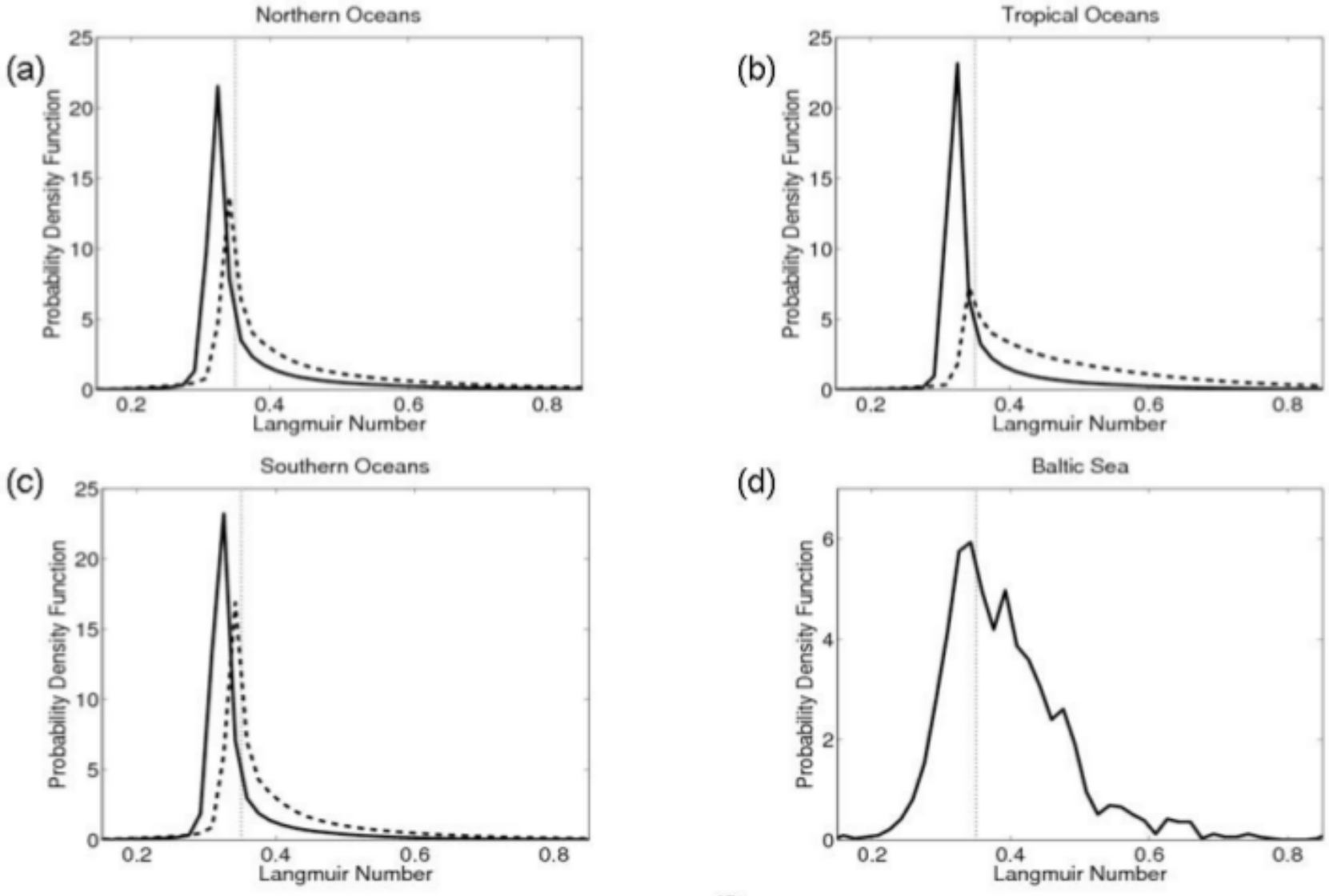

Climatological histograms in several regions of Langmuir number, $La = \sqrt{u_*/U^{st}}$. The gray line indicates the authors' estimate of the Wind-Wave Equilibrium value of $La = 0.35$. The usual state of the oceanic surface boundary layer is some form of Langmuir Turbulence, but disequilibrium is not uncommon. Solid and black lines are different time periods. (Belcher *et al.*, 2012)

References

Belcher *et al.*, 2012: A global perspective on Langmuir turbulence in the ocean surface boundary layer. *Geophys. Res. Lett.* **39**, L18605.

Craik, A., and S. Leibovich, 1976: A rational model for Langmuir circulations. *J. Fluid Mech.* **73**, 401-426.

de Boyer Montegut, C., G. Madec, A. S. Fischer, A. Lazar, and D. Iudicone, 2004: Mixed layer depth over the global ocean: an examination of profile data and a profile-based climatology. *J. Geophys. Res.* **109**, C12003, doi:10.1029/2004JC002378.

Brainerd, K.E. and Gregg, M.C., 1993: Diurnal restratification and turbulence in the oceanic surface mixed layer 1. Observations. *J. Geophys. Res.* **98**, 22645-22656.

Kalnay, E. and many co-authors, 1996: The NCEP/NCAR 40-year reanalysis project. *Bull. Amer. Met. Soc.* **77**, 437-471.

Large, W. and S. Yeager, 2009: The global climatology of an interannually varying air-sea flux data set. *Climate Dyn.* **33**, 341-364.

McWilliams, J.C., & J.M. Restrepo, 1999: The wave-driven ocean circulation. *J. Phys. Ocean.* **29**, 2523-2540.

Niiler, P.P., 1992: The ocean circulation. In: *Climate System Modeling*, K. Trenberth (ed.), Cambridge University Press, 117-148.

Ralph, E.A., and P.P. Niiler, 1999: Wind-driven currents in the tropical Pacific. *J. Phys. Ocean.* **29**, 2121-2129.

Sullivan, P.P., and J.C. McWilliams, 2010: Dynamics of winds and currents coupled to surface waves. *Ann. Rev. Fluid Mech.* **42**, 19-42.